

# Increasing the Brønsted Acidity of Flame-Derived Silica/Alumina up to Zeolitic Strength\*\*

Jun Huang, Niels van Vegten, Yijiao Jiang, Michael Hunger, and Alfons Baiker\*

Solid acids facilitate cleaner and much easier reactions and thus have replaced toxic, corrosive, and unrecyclable liquid mineral acids in many catalytic applications, the most prominent being the cracking and refining of a billion tons of crude oil into useful chemical components.<sup>[1,2]</sup> For current global challenges involving energy sources and environmentally friendly processes,<sup>[3,4]</sup> chemists and engineers strive towards designing improved solid acids because of their dominant role in renewable fuels generation and application in clean chemical processes.<sup>[2,5,6]</sup> The desired solid acids should have tunable properties to offer optimal acidity for efficient catalysis of the target reactions. Amorphous silica/alumina (SA) is one of the popular solid acids that provide moderate Brønsted acidity, albeit weaker than that of zeolites.<sup>[7]</sup> SAs have been directly used as an important acid catalyst in oil refineries and, furthermore, have been applied as excellent supports for nanoparticles in many hydrogenation and oxidation reactions.<sup>[8]</sup> Current efforts are aimed at enhancing the Brønsted acidity of SAs so that they are close or ideally similar in strength to that of zeolites.<sup>[9–12]</sup> Herein, we show that SAs prepared by flame-spray pyrolysis (FSP SAs) exhibit a strong Brønsted acidity resembling that of zeolites. Some Brønsted acid sites in the FSP SAs were found to be even stronger than those of H-ZSM-5, which is regarded as the most acidic zeolite.

Brønsted acidity of SAs is generated by having neighboring aluminum and silanol groups. However, inhomogeneous composition of the SAs resulting from existing preparation methods, such as cogelation, grafting, co-precipitation, and hydrolysis, hinder enhancement of their acidity. Control over pH values and high temperature calcinations are often required in these methods for the diffusion of aluminum and silicon throughout the phase or network.<sup>[13]</sup> FSP allows production of thermally stable nanoparticles in a single step, and currently pilot-plant-scale reactions have been accomplished, approaching a production rate of 500 g h<sup>-1</sup>, thus showing potential for industrial applications.<sup>[14]</sup> FSP allows

the production of SAs from its dissolved precursors within a few milliseconds, and promotes the homogeneous composition and formation of Al–O–Si bonds. Furthermore, transition- and noble-metal components can be added to the precursor solutions thereby enabling the direct synthesis of SA-supported metal catalysts.<sup>[15–17]</sup>

Herein, we show that the obtained SAs have tunable Brønsted acidities ranging from moderate to zeolitic acid strength, depending on the aluminum content, thereby allowing their versatile utilization in chemical industry. Solid-state NMR analysis is a powerful method for characterizing surface acidity, accessibility, and the local structure of Brønsted acid sites in a direct manner.<sup>[18–30]</sup> By applying multinuclear solid-state NMR spectroscopy we investigated surface density, strength, and accessibility of acidic OH groups in FSP SAs and elucidated the relationship between Brønsted acidity and local silicon–aluminum coordination.

Silica/alumina particles were prepared by the spray combustion of precursor solutions containing aluminum acetylacetonate and tetraethoxysilane in a methanol/acetic acid (1:1) mixture. The solution was nebulized by a flow of oxygen and ignited by an annular methane/oxygen flame. The obtained silica/alumina having 0, 10, 30, 50, 70, and 90 atom % of aluminum were denoted as FSP SA/0, 10, 30, 50, 70, and 90, respectively. Their surface areas, determined by N<sub>2</sub> adsorption, were between 156 and 377 m<sup>2</sup> g<sup>-1</sup> and are summarized in Table S1 in the Supporting Information.

Firstly, the acidic properties of FSP-made SiO<sub>2</sub> (FSP SA/0) was investigated. After dehydration of FSP SA/0 at 673 K, the <sup>1</sup>H MAS NMR spectrum (Figure 1 a) consisted of a strong signal at  $\delta_{\text{H}} = 1.8$  ppm, which was assigned to silanol groups, and a shoulder at  $\delta_{\text{H}} = 2.6$  ppm resulting from hydrogen-bonded silanol groups. Most of these silanols are Si(OSi)<sub>3</sub>OH species as evidenced by <sup>29</sup>Si MAS NMR spectroscopy (see Figure S1 in the Supporting Information). The dominating Q<sup>4</sup> species (Si(OSi)<sub>4</sub>) having a signal at  $\delta = -110$  ppm and the Q<sup>3</sup> species (Si(OSi)<sub>3</sub>OH) having a signal at  $\delta_{\text{H}} = -101$  ppm were observed along with the Q<sup>2</sup> species (Si(OSi)<sub>2</sub>(OH)<sub>2</sub>), which had a corresponding weak peak at  $\delta = -90$  ppm. The silanol groups of the Q<sup>3</sup> species have greater acid strength than those of the Q<sup>2</sup> and Q<sup>0</sup> species.<sup>[31]</sup> After loading the weak base, CD<sub>3</sub>CN, onto the surface, hydrogen bonds were formed between the probe molecules and the silanol groups, thereby leading to a low-field shift of the <sup>1</sup>H NMR signal from  $\delta_{\text{H}} = 1.8$  to 4.8 ppm (Figure 1 c). Since larger low-field shifts indicate stronger acidic sites, the acid strength of silanol in FSP SA/0 ( $\Delta\delta_{\text{H}} = 3$  ppm) is weaker than that of the bridging OH groups in zeolite H-X ( $\Delta\delta_{\text{H}} = 3.6$  ppm) and H-Y ( $\Delta\delta_{\text{H}} = 5.1$  ppm).<sup>[32]</sup> The acidic sites in FSP-made SiO<sub>2</sub> were not capable of protonating adsorbed ammonia (Figure 1 b), as

[\*] Dr. J. Huang, N. van Vegten, Dr. Y. Jiang, Prof. Dr. A. Baiker  
Institute of Chemical and Bioengineering, ETH Zürich  
Hönggerberg, HCI, 8093 Zürich (Switzerland)  
Fax: (+41) 44-632-1163  
E-mail: baiker@chem.ethz.ch  
Homepage: <http://www.baiker.ethz.ch>  
Prof. Dr. M. Hunger  
Institute of Chemical Technology, Universität Stuttgart (Germany)

[\*\*] We kindly acknowledge financial support by the ETH, Zürich (no. TH-09 06-2).

Supporting information for this article is available on the WWW under <http://dx.doi.org/10.1002/anie.201003391>.

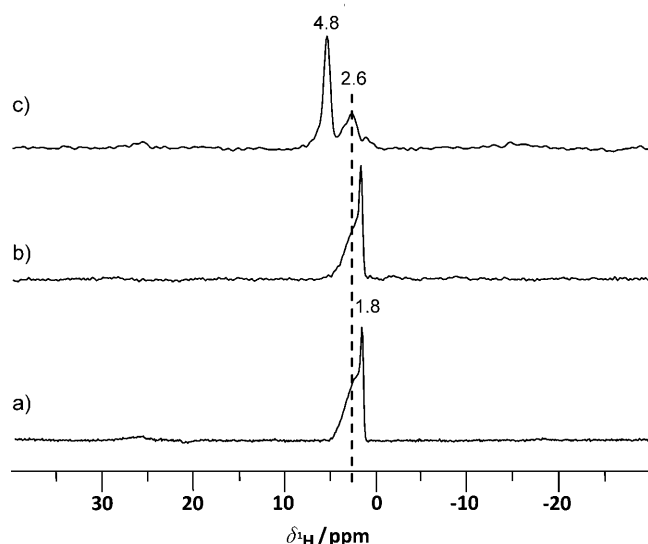


**Figure 1.**  $^1\text{H}$  MAS NMR spectra of a) FSP SA/0 dehydrated at 673 K, b) sample (a) after loading with  $\text{NH}_3$  and evacuation at 373 K for 1 h, and c) sample (a) after loading with  $\text{CD}_3\text{CN}$  and evacuation at RT for 1 h. MAS = magic-angle spinning.

determined by the absence of a signal at approximately  $\delta = 7$  ppm (ammonium ions) in the  $^1\text{H}$  MAS NMR spectra after adsorption of ammonia and subsequent evacuation at 373 K.

Upon addition of aluminum during flame synthesis, the surface structure of the obtained FSP SAs changed was altered. Hydrogen bonds between the silanol groups did not exist in this case, as indicated by the disappearance of the shoulder at  $\delta = 2.6$  ppm in the  $^1\text{H}$  MAS NMR spectrum of dehydrated FSP SA/10 (Figure 2a). This finding is attributed to aluminum atoms which were located in the vicinity of the SiOH groups, thereby blocking the interaction between the silanol groups. Simultaneously, the  $^{29}\text{Si}$  MAS NMR spectra in Figure S1 of the Supporting Information shows a low-field shift of the main peaks, thus hinting at a substitution of the silicon sites by aluminum atoms, even in the vicinity of silanol groups ( $\text{Si}(\text{OAl})(\text{OSi})_2\text{OH}$ ). As a result of this aluminum incorporation, the acid strength of the silanol groups was enhanced. Unlike the zeolite crystals, however, the aluminum incorporation in the vicinity of the silanol groups in SA did not affect the  $^1\text{H}$  MAS NMR shift for the non-interacting SiOH groups; however, a change in the shift was obvious upon adsorption of the basic probe molecules.

Adsorption of the strongly basic probe molecule  $\text{NH}_3$  was performed on dehydrated samples at room temperature. After evacuation of weakly adsorbed  $\text{NH}_3$ , the  $^1\text{H}$  MAS NMR spectrum of dehydrated FSP SA/10 (Figure 2b) showed two new peaks at approximately  $\delta = 4.0$  and  $7.0$  ppm. The broad signal at  $\delta = 4.0$  ppm is attributed to  $\text{NH}_3$  that is hydrogen bonded to the weakly acidic silanol groups, which can be completely removed after evacuation at 373 K for 1 hour (Figure 2c). The signal at approximately  $\delta = 7.0$  ppm results from the formation of ammonium ions generated by the protonation of  $\text{NH}_3$  at the strong Brønsted acid sites. These ammonium ions have a high thermal stability and can be utilized for quantifying the number of strongly acidic sites.

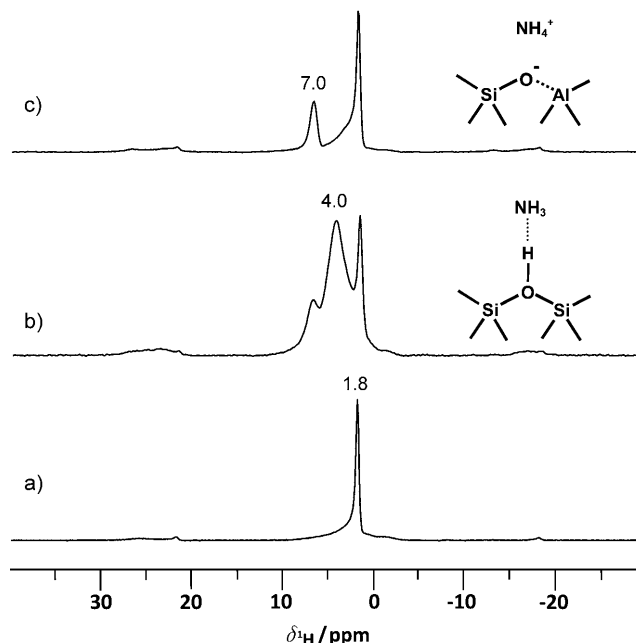


**Figure 2.**  $^1\text{H}$  MAS NMR spectra of dehydrated (673 K) FSP SA/10 (a) and FSP SA/10 loaded with  $\text{NH}_3$  (b). c)  $^1\text{H}$  MAS NMR spectra of sample in (b) evacuated at 373 K in 1 h.

Therefore,  $^1\text{H}$  MAS NMR investigations were carried out for all dehydrated FSP SAs after adsorption of ammonia and evacuation at 373 K. The values for quantification of the strongly acidic sites were obtained by evaluating the intensity of the signal at approximately  $\delta = 7$  ppm which resulted from the formation of ammonium ions at these strongly acidic sites (Table 1, columns 3 and 4). The values for the quantification of the weakly acidic sites were calculated from the number of silanol groups having no neighboring aluminum and interacting with ammonia through hydrogen bonds (Table 1, column 2). As shown in Figures 2 and 3, the intensity of the peak at approximately  $\delta = 7$  ppm increased with an increase in the aluminum content from 10 to 70 %. Upon additional increases in the aluminum content, the intensity of this signal decreased. This observation indicates that the number of strongly acid sites on the FSP-made silica/alumina can be tuned by the aluminum content, as is also well known for

**Table 1:** Molar fraction and concentration of strong and weak Brønsted acid sites on FSP SAs.<sup>[a]</sup>

FSP SAs	Weakly acidic OH groups: molar fraction [%]	Strongly acidic OH groups: molar fraction [%]	Strongly acidic OH groups: population density [mmol g <sup>-1</sup> ]
FSP SA/10	42.3	7.7	$9.8 \times 10^{-2}$
FSP SA/30	35.5	9.6	$11.1 \times 10^{-2}$
FSP SA/50	33.0	12.7	$13.4 \times 10^{-2}$
FSP SA/70	8.3	13.0	$15.1 \times 10^{-2}$
FSP SA/90	1.6	5.5	$5.7 \times 10^{-2}$

[a] The molar fractions are related to the total number of hydroxy groups, including non-acidic AlOH groups.

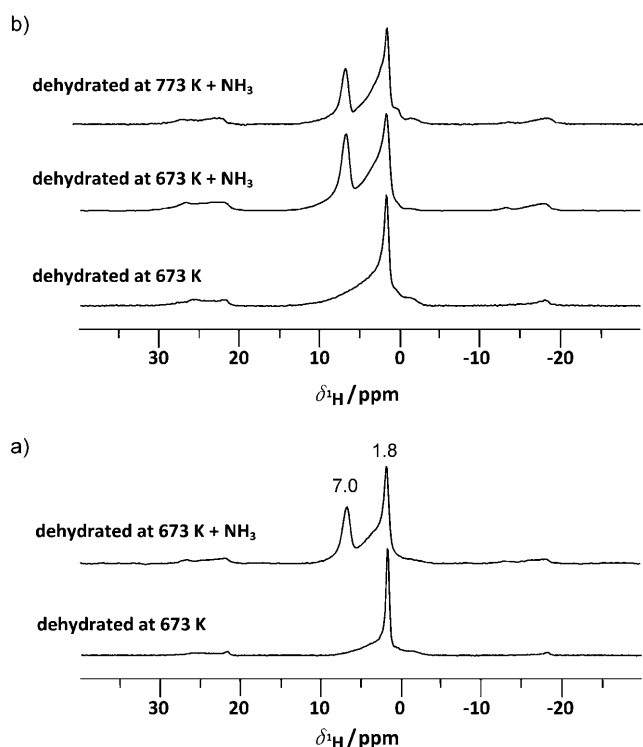


**Figure 3.**  $^1\text{H}$  MAS NMR spectra of dehydrated FSP SA/30 (a) and SA/70 (b) recorded before and after loading with  $\text{NH}_3$  and subsequent evacuation of  $\text{NH}_3$  loaded samples at 373 K for 1 h.

classical solid acids made of aluminum and silicon containing mixed oxides.<sup>[1,2]</sup>

Generally, three types of OH groups on the FSP SAs surface can be assumed: 1) non-acidic AlOH groups (no shifts after loading  $\text{CD}_3\text{CN}$ ), 2) weakly acidic silanol groups, and 3) strong Brønsted acid sites (silanols with neighboring aluminum species). The molar ratio of strongly acidic sites (Table 1, column 3) increases from 7.7% for FSP SA/10 to 13.0% for FSP SA/70. The residual OH groups are either non-acidic or weakly acidic. The molar fraction of weakly acidic silanol groups decreases strongly from 42.3 to 1.6% with increasing aluminum content from 10 to 90% (Table 1, column 2). By adjusting the aluminum content, FSP SAs either having a few but predominantly strong Brønsted acid sites or having a few strong Brønsted acid sites and about five times the number of weakly acidic sites can be obtained.

In addition, the molar ratio of acid sites can be controlled by varying the dehydration temperatures. As shown in Figure 3b, the number of strongly acid sites (causing the signal of the ammonium ions at  $\delta = 7$  ppm) and non-acidic AlOH groups at approximately  $\delta = 2.6$  ppm decreased with increasing dehydration temperature in the range of 673 to 773 K. It means that protons from strongly acid sites in combination with nearby AlOH groups form water molecules which were removed from the FSP SAs by evacuation at elevated temperature. The weakly acidic silanol groups still remained, thus reducing the molar ratio of strongly acid sites. The above-mentioned tunable properties of FSP SAs may have great application potential in chemical industry. Take

petroleum cracking for example, the combination of predominantly weak Brønsted acid sites with relatively few strong sites in catalysts can lead to high gasoline yields with low selectivity to olefins and relatively high coke formation, because of extensive hydrogen transfer.<sup>[33]</sup> Alternatively, catalysts with relatively few but predominantly strong Brønsted acid sites generally result in less gasoline but more olefins with lower coke formation.

As shown in column 4 of Table 1, Brønsted acidity reaches a maximum on FSP SA at about 70% aluminum. This value is quite different from that for amorphous silica/alumina prepared by other methods, wherein maximum Brønsted acidity is attained at around 30% aluminum.<sup>[1]</sup> It is well known that the acidity of silica/alumina strongly depends upon the local structure of surface sites on the material. A double-resonance  $^1\text{H}/^{27}\text{Al}$ TRAPDOR (transfer of population in double resonance) NMR technique is often applied to probe the Si–O–Al connectivity in solid acids composed of silicon and aluminum.<sup>[34]</sup> Through  $^1\text{H}/^{27}\text{Al}$ TRAPDOR MAS NMR results for FSP SA/70, the dipolar coupling between protons and aluminum nuclei was observed. The difference spectrum of  $^1\text{H}$  spin-echo MAS NMR spectra with and without  $^{27}\text{Al}$  irradiation is shown in Figure 4. A strong signal at  $\delta = 1.8$  ppm was

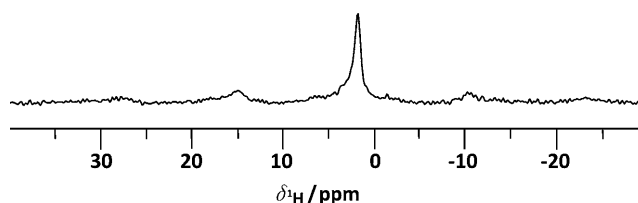


**Figure 4.**  $^1\text{H}/^{27}\text{Al}$ TRAPDOR MAS NMR difference spectrum of FSP SA/70 dehydrated at 673 K.

detected and represents the silanol groups interacting with nearby aluminum species. Their interaction is considered to contribute to strong Brønsted acidity. The widely accepted opinion is that tetrahedrally coordinated aluminum neighboring silanol groups causes this Brønsted acidity. For FSP SAs in this investigation, however, this correlation was not observed (see Table 1). Therefore,  $^{27}\text{Al}$  and  $^{29}\text{Si}$  MAS NMR investigations were carried out to understand the relationships between the local structure of the acid sites and the acidity of the FSP SAs.

Some  $^{27}\text{Al}$  MAS NMR spectra of FSP SAs are shown in Figure 5. In FSP SA/10, a large number of aluminum atoms are tetrahedrally coordinated ( $\text{Al}^{\text{IV}}$ ), which results in the  $^{27}\text{Al}$  MAS NMR signal occurring at  $\delta = 60$  ppm. A weak signal at  $\delta = 5$  ppm is attributed to a small amount of octahedrally coordinated aluminum ( $\text{Al}^{\text{VI}}$ ). For FSP SA/30 (30 mol % Al), the pentacoordinated aluminum ( $\text{Al}^{\text{V}}$ ) was observed and gave rise to a new signal at approximately  $\delta = 35$  ppm. Upon increasing the aluminum content to 70 mol %, the intensity of  $\text{Al}^{\text{V}}$  peak is increased and accompanied by an increase of the molar ratio of strongly acidic sites, but the molar ratios of  $\text{Al}^{\text{IV}}$  to  $\text{Al}^{\text{V}}$  are lowered (see data in Table S1 in the Supporting Information). As previously described, only

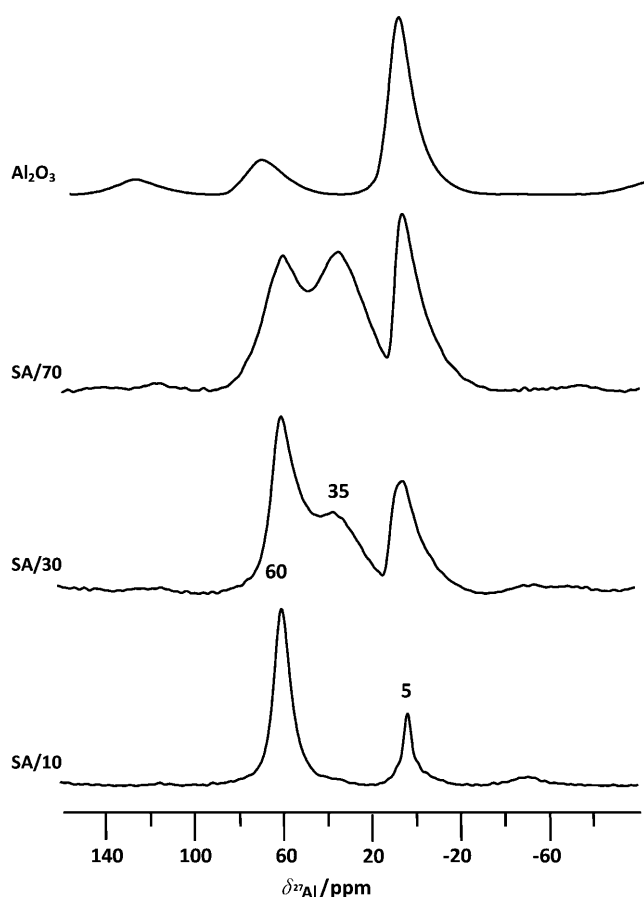


Figure 5.  $^{27}\text{Al}$  MAS NMR spectra of FSP SA/10, 30, 70, and alumina.

silanol having neighboring aluminum centers can exhibit strongly acidic sites; that is, there is a correlation between  $\text{Al}^{\text{V}}$  and strongly acidic sites. Surprisingly, a narrow signal at  $\delta = -80$  ppm occurs in  $^{29}\text{Si}$  solid-state NMR spectra of FSP SA/30 (see Figure S1 in the Supporting Information and Figure 6). To our knowledge, this signal has never been observed for amorphous silica/alumina that has been prepared by other methods. It means that there might be a new type of interaction between the aluminum and silicon atoms in FSP SAs, and interaction that may correspond to the specific Brønsted acid sites.

$\text{Al}^{\text{V}}$  was observed as an extra-framework species ( $\text{Al}(\text{OH})_3 \cdot 2\text{H}_2\text{O}$  or  $\text{Al}(\text{OH})_2 \cdot 3\text{H}_2\text{O}$ ) after dealumination of zeolites.<sup>[35,36]</sup> These species can be dehydrated to low-coordinated aluminum cations such as  $\text{AlOOH}$ ,  $\text{AlO}^+$ ,  $\text{Al}(\text{OH})^{2+}$ ,  $\text{Al}(\text{OH})^{2+}$ , and  $\text{Al}^{3+}$ , which are able to enhance the acid strength of neighboring bridging OH groups.<sup>[18,37]</sup> In zeolites, a high aluminum content in the framework will reduce the acid strength of bridging OH groups because of the change in electronegativity.<sup>[7]</sup> In amorphous silica/alumina, the formation of Brønsted acid sites is different to that in crystalline zeolites. The Brønsted acidity is generated by silanol groups, which are strongly influenced by neighboring aluminum.<sup>[2]</sup> FSP provides a homogeneous distribution of silicon throughout an alumina-rich matrix, which promotes the formation of silanol groups having neighboring aluminum centers and causes a narrow signal at  $\delta = -80$  ppm in  $^{29}\text{Si}$  solid-state NMR

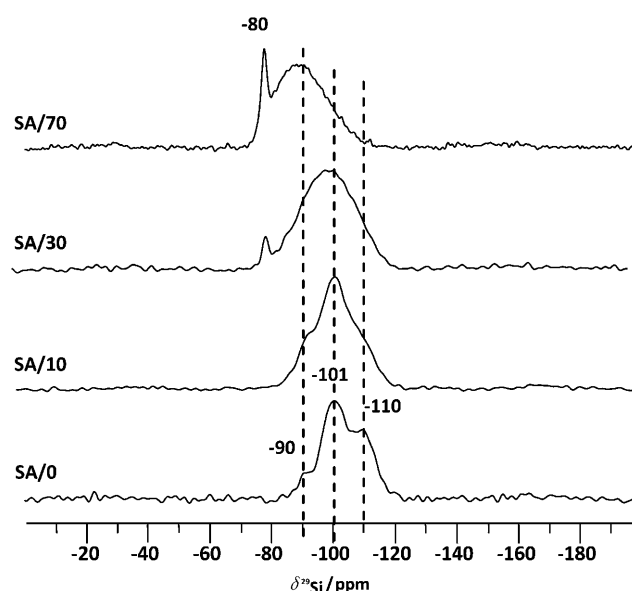
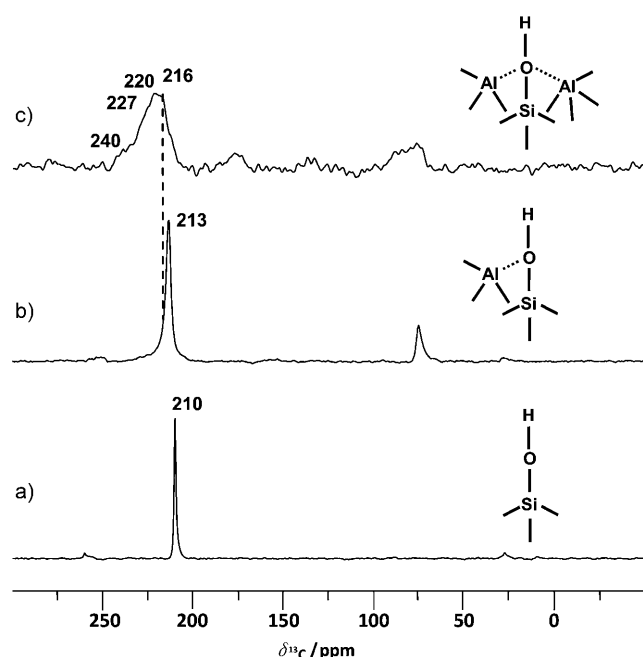


Figure 6.  $^{29}\text{Si}$  CP/MAS NMR spectra of FSP SA/0, 10, 30, and 70.

spectra. The more aluminum that is located around silanol groups will induce a strong transfer of electron density from the OH groups and generate very strong acid sites.

Ammonia is a relatively strong base, which cannot distinguish between Brønsted acid sites with different acid strengths, whereas acetone ( $\text{CH}_3^{13}\text{COCH}_3$ ) is a suitable probe molecule and widely used for this type of investigation.<sup>[38]</sup> The adsorbate-induced low-field shift ( $\Delta\delta_{13\text{C}}$ ) of acetone upon interaction with solid acids is a well-accepted scale for acid strength. Figure 7 presents  $^{13}\text{C}$  MAS NMR spectra of dehydrated (673 K) FSP SAs recorded after loading acetone. For FSP SA/0, the interaction between weak acidic silanol groups (Figure 7b) and carbonyl groups of acetone gives a narrow signal at  $\delta = 210$  ppm. For FSP SA/10, most of the tetrahedrally coordinated aluminum is in the vicinity of silanol groups (Figure 7a), which enhances the acid strength. These single Al-O types of interactions in FSP SA/10 induced a strong peak at  $\delta = 213$  ppm after adsorption of acetone. When the aluminum content was higher than 30 %, a wide distribution of acid strengths was observed and led to signals between  $\delta = 216$  and 230 ppm after adsorption of acetone. In Figure 7c, a shoulder at  $\delta = 240$  ppm in the  $^{13}\text{C}$  MAS NMR spectrum resulted from the acetone adsorbed onto the Lewis acidic alumina in FSP SA/70. This signal was difficult to observe in FSP SA/10, since nearly no surface Lewis acidic sites were generated.

The data in Table 2 show a comparison between the chemical shifts ( $\delta_{13\text{C}}$ ) and low-field shifts ( $\Delta\delta_{13\text{C}}$ ) of  $[2-^{13}\text{C}]$ acetone interacting with the acidic protons of FSP SAs and zeolites. FSP SA/10 possesses moderate acidity that is sufficient to protonate ammonia, but it is still weaker than that of zeolites. FSP SA/70 showed peaks at  $\delta_{13\text{C}} = 216$ , 220, and 227 ppm corresponding to  $\Delta\delta_{13\text{C}} = 11$ , 15, and 22 ppm, respectively. These values are similar or even higher than those of zeolites H-X, H-Y, and ZSM-5, indicating that FSP SAs can provide stronger Brønsted acid sites than ZSM-5 (the most acidic zeolite). The presence of such



**Figure 7.**  $^{13}\text{C}$  MAS NMR spectra of dehydrated (673 K) FSP SA/0 (a); SA/10 (b); and SA/70 recorded after loading and evacuation of  $[2\text{-}^{13}\text{C}]\text{acetone}$  (c).

**Table 2:** Resonance positions ( $\delta_{13\text{C}}$ ) and low-field shifts ( $\Delta\delta_{13\text{C}}$ ) of  $[2\text{-}^{13}\text{C}]\text{acetone}$  adsorbed at the Brønsted acid sites of FSP SAs and zeolites.

Acids	$\delta_{13\text{C}}$	$\Delta\delta_{13\text{C}}$	Ref.
$\text{CDCl}_3$	205	0	[38]
FSP SA/0	210	5	this work
FSP SA/10	213	8	this work
H-X	215	10	[38]
H-Y	220	15	[38]
ZSM-5	223	18	[38, 39]
FSP SA/70	216, 220, 227	11, 15, 22	this work
FSP SA/90	230	25	this work

strong Brønsted acid sites was additionally evidenced by temperature-programmed desorption (TPD) of  $\text{NH}_3$ , as described in the Supporting Information. TPD curves in Figure S2 show a strong high-temperature peak (350–550 °C) for FSP SA/70 and zeolite H-ZSM-5.

We attribute this to the presence of the  $\text{Al}^{\text{V}}$  species in FSP SAs. Pentacoordinated aluminum has been assigned to an interface species between alumina and a mixed silica/alumina phase or between an alumina-type phase and a mixed silica/alumina phase.<sup>[40]</sup> Therefore,  $\text{Al}^{\text{V}}$  species are in proximity to silicon in part of the alumina network, and causes the narrow signal at  $\delta = -80$  ppm and low-field shifts of other board peaks in the  $^{29}\text{Si}$  MAS NMR spectra. If  $\text{Al}^{\text{V}}$  species are close to silanol groups, they can generate a “pseudo-bridging silanol” and enhance the acidity.<sup>[9]</sup> If  $\text{Al}^{\text{V}}$  species are located in the surroundings of relatively strong Brønsted acid sites (Figure 7c), the acid strength will be additionally increased to be similar or stronger than those in zeolites.

In summary, flame-spray pyrolysis provides a single-step preparation method combining synthesis and calcinations, and yields silica/alumina in milliseconds. We have elucidated the specific surface structure and Al–O–Si bonds of FSP SAs by using  $^{29}\text{Si}$  and  $^{27}\text{Al}$  solid-state NMR methods. The obtained data as it relates to their Brønsted acidity. After adsorption of probe molecules, the accessibility of Brønsted acid sites in FSP SAs was demonstrated by  $^1\text{H}$  and  $^{13}\text{C}$  MAS NMR spectroscopy. These sites having different acid strengths were additionally distinguished and quantified. Silanol groups without neighboring aluminum centers are weak acid sites. Tetrahedrally coordinated aluminum in the vicinity of silanol groups results in moderate Brønsted acidity for FSP SA/10 as compared to that of zeolites. When moderate acid sites interact with nearby pentacoordinated aluminum species, extra pseudo-bridging bonds are generated. This enhances their Brønsted acidity to strengths that are similar or even higher than those encountered in zeolites. The population density of these strong Brønsted acid sites reached  $15.15 \times 10^{-2} \text{ mmol g}^{-1}$  for FSP SA/70, and the molar ratio of strong and weak acid sites can be easily adjusted for desired reactions by varying the aluminum content. These tunable acid properties of FSP SAs may promote its application as a solid acid and as an acidic support in chemical industry. Additional investigations on their catalytic applications are in progress.

## Experimental Section

Aluminum(III) acetylacetonate (99%, ABCR), tetraethoxysilane (99%, Fluka) acetic acid (analytical grade, Fluka) and methanol (analytical grade, Fluka) were used as received. The experimental setup used for the flame-spray pyrolysis (FSP) has been described in detail elsewhere.<sup>[14]</sup> In brief, FSP-made silica/alumina (SA) catalysts were prepared by dissolving the appropriate amount of the precursor materials in a 1:1 (vol %) mixture of acetic acid and methanol. The resulting solution was filtered using a glass filter, pumped through a capillary at a rate of  $5 \text{ mL min}^{-1}$ , and nebulized at  $5 \text{ L min}^{-1} \text{ O}_2$ . The resulting spray was ignited by an annular supporting methane/oxygen flame ( $1.5/0.9 \text{ L min}^{-1}$ ), resulting in an approximately 6 cm long flame. Particles were collected on a cooled Whatman GF6 filter (257 mm diameter). A Busch SV 1040C vacuum pump aided in particle recovery.

FSP SAs were dehydrated at 673 K in vacuum at pressure  $p < 10^{-2}$  mbar for 4 h. Subsequently, the samples were sealed or immediately used for in situ loading.  $[\text{D}_3]\text{Acetonitrile}$  (99.9% deuterated) and  $[2\text{-}^{13}\text{C}]\text{acetone}$  (99.5%  $^{13}\text{C}$ -enriched) were purchased from Acro and Sigma–Aldrich, respectively. The dehydrated FSP SAs were quantitatively loaded with one probe molecule of  $\text{NH}_3$ ,  $\text{CD}_3\text{CN}$ , and  $\text{CH}_3^{13}\text{COCH}_3$  per OH group and, subsequently, evacuated at 373 K or RT for removing weakly hydrogen-bonded or physisorbed compounds. Samples were filled into MAS NMR rotors in a glove box under dry nitrogen gas. The details of solid-state NMR measurements are described in the Supporting Information.

Received: June 4, 2010

Published online: September 6, 2010

**Keywords:** Brønsted acidity · flame-spray pyrolysis · NMR spectroscopy · silica/alumina · solid-state structures



- [1] K. Tanabe, *Solid Acids and Bases and Their Catalytic Properties*, Academic Press, New York, **1970**.
- [2] G. Busca, *Chem. Rev.* **2007**, *107*, 5366.
- [3] M. I. Hoffert, K. Caldeira, G. Benford, D. R. Criswell, C. Green, H. Herzog, A. K. Jain, H. S. Kheshgi, K. S. Lackner, J. S. Lewis, H. D. Lightfoot, W. Manheimer, J. C. Mankins, M. E. Mauel, L. J. Perkins, M. E. Schlesinger, T. Volk, T. M. L. Wigley, *Science* **2002**, *298*, 981.
- [4] M. S. Dresselhaus, I. L. Thomas, *Nature* **2001**, *414*, 332.
- [5] M. Stöcker, *Angew. Chem.* **2008**, *120*, 9340; *Angew. Chem. Int. Ed.* **2008**, *47*, 9200.
- [6] G. W. Huber, S. Iborra, A. Corma, *Chem. Rev.* **2006**, *106*, 4044.
- [7] A. Corma, *Chem. Rev.* **1995**, *95*, 559.
- [8] G. Ertl, H. Knözinger, F. Schüth, J. Weitkamp, *Handbook of Heterogeneous Catalysis*, 2<sup>nd</sup> ed., Wiley-VCH, Weinheim, **2008**.
- [9] C. Chizallet, P. Raybaud, *Angew. Chem.* **2009**, *121*, 2935; *Angew. Chem. Int. Ed.* **2009**, *48*, 2891.
- [10] B. Xu, C. Sievers, J. A. Lercher, J. A. R. van Veen, P. Giltay, R. Prins, J. A. van Bokhoven, *J. Phys. Chem. C* **2007**, *111*, 12075.
- [11] G. Sartori, R. Maggi, *Chem. Rev.* **2006**, *106*, 1077.
- [12] E. J. M. Hensen, D. G. Poduval, P. C. M. M. Magusin, A. E. Coumans, J. A. R. v. Veen, *J. Catal.* **2010**, *269*, 201.
- [13] J. Scherzer, A. J. Gruia, *Hydrocracking Science and Technology*, Marcel Dekker, New York, **1996**.
- [14] R. Stöbel, A. Baiker, S. E. Pratsinis, *Adv. Powder Technol.* **2006**, *17*, 457.
- [15] N. van Vegten, M. Maciejewski, F. Krumeich, A. Baiker, *Appl. Catal. B* **2009**, *93*, 38.
- [16] R. Büchel, R. Stöbel, A. Baiker, S. E. Pratsinis, *Top. Catal.* **2009**, *52*, 1799.
- [17] B. Schimmoeller, F. Hoxha, T. Mallat, F. Krumeich, S. E. Pratsinis, A. Baiker, *Appl. Catal. A* **2010**, *374*, 48.
- [18] S. H. Li, A. M. Zheng, Y. C. Su, H. L. Zhang, L. Chen, J. Yang, C. H. Ye, F. Deng, *J. Am. Chem. Soc.* **2007**, *129*, 11161.
- [19] M. Haouas, S. Walspurger, F. Taulelle, J. Sommer, *J. Am. Chem. Soc.* **2004**, *126*, 599.
- [20] J. Trébosc, J. W. Wiench, S. Huh, V. S. Y. Lin, M. Pruski, *J. Am. Chem. Soc.* **2005**, *127*, 3057.
- [21] J. Kanellopoulos, C. Gottert, D. Schneider, B. Knorr, D. Prager, H. Ernst, D. Freude, *J. Catal.* **2008**, *255*, 68.
- [22] J. Weitkamp, M. Hunger, *Stud. Surf. Sci. Catal.* **2007**, *168*, 787.
- [23] L. M. Peng, C. P. Grey, *Microporous Mesoporous Mater.* **2008**, *116*, 277.
- [24] A. G. Stepanov, S. S. Arzurnanov, M. V. Luzgin, H. Ernst, D. Freude, V. N. Parmon, *J. Catal.* **2005**, *235*, 221.
- [25] A. Simperler, R. G. Bell, M. W. Anderson, *J. Phys. Chem. B* **2004**, *108*, 7142.
- [26] J. F. Haw, T. Xu, J. B. Nicholas, P. W. Goguen, *Nature* **1997**, *389*, 832.
- [27] C. Collins, G. Mann, E. Hoppe, T. Duggal, T. L. Barr, J. Klinowski, *Phys. Chem. Chem. Phys.* **1999**, *1*, 3685.
- [28] E. M. El-Malki, R. A. van Santen, W. M. H. Sachtler, *J. Phys. Chem. B* **1999**, *103*, 4611.
- [29] C. Pazé, A. Zecchina, S. Spera, G. Spano, F. Rivetti, *Phys. Chem. Chem. Phys.* **2000**, *2*, 5756.
- [30] G. Crépeau, V. Montouillout, A. Vimont, L. Mariey, T. Cseri, F. Mauge, *J. Phys. Chem. B* **2006**, *110*, 15172.
- [31] J. M. Rosenholm, T. Czuryzkiewicz, F. Kleitz, J. B. Rosenholm, M. Linden, *Langmuir* **2007**, *23*, 4315.
- [32] J. Huang, Y. Jiang, V. R. R. Marthala, B. Thomas, E. Romanova, M. Hunger, *J. Phys. Chem. C* **2008**, *112*, 3811.
- [33] G. Ertl, H. Knözinger, J. Weitkamp, *Handbook of Heterogeneous Catalysis*, Wiley-VCH, Weinheim, **1997**.
- [34] M. Hunger, W. Wang, *Adv. Catal.* **2006**, *50*, 149.
- [35] C. A. Fyfe, J. L. Bretherton, L. Y. Lam, *J. Am. Chem. Soc.* **2001**, *123*, 5285.
- [36] J. Kanellopoulos, A. Unger, W. Schwieger, D. Freude, *J. Catal.* **2006**, *237*, 416.
- [37] C. J. A. Mota, D. L. Bhering, N. Rosenbach, Jr., *Angew. Chem.* **2004**, *116*, 3112; *Angew. Chem. Int. Ed.* **2004**, *43*, 3050.
- [38] J. F. Haw, J. B. Nicholas, T. Xu, L. W. Beck, D. B. Ferguson, *Acc. Chem. Res.* **1996**, *29*, 259.
- [39] A. M. Zheng, H. L. Zhang, L. Chen, Y. Yue, C. H. Ye, F. Deng, *J. Phys. Chem. B* **2007**, *111*, 3085.
- [40] M. F. Williams, B. Fonfe, C. Sievers, A. Abraham, J. A. van Bokhoven, A. Jentys, J. A. R. van Veen, J. A. Lercher, *J. Catal.* **2007**, *251*, 485.